8th International Symposium on Magnetic Bearing
August 26-28, 2002, Mito, Japan

Motion and Vibration Control of Flexible Rotor Using Magnetic Bearings

Hideo Shida, Mitsuhiro Ichihara and Kazuto Seto
Seto Lab., Department of Mechanical Engineering, College of Science & Technology,
Nihon University, Kanda Surugadai 1-8, Chiyoda-ku, Tokyo 101-8308, Japan

Muneharu Saigo
National Institute of Advanced Industrial Science and Technology, Central 2, 1-1-1, Umezono,
Tsukuba, Ibarakai 305-8568, Japan

ABSTRACT

This paper deals with a new design procedure for controlling a flexible rotor system using active magnetic bearings (AMB).

The research aim is to satisfactorily pass through a critical speed and achieve high-speed rotation. For this purpose, it is necessary to control both vibration and motion using the modeling method presented in Seto[1] and an effective control method. Furthermore, utilizing the model, the design of a new controller consisting of the combination of PID control and LQ control is applied to the control of motion and vibrations of a flexible rotor.

Computer simulations are carried out and the effectiveness of the presented procedure is investigated.

1. INTRODUCTION

In recent years, AMB systems have been applied to various machines such as grinding machines and energy storage flywheel systems. In general, these control systems include a notch-filter or consider only the control of the first three modes. Furthermore, in the case of an unforeseen accident, because the transfer function changes, the notch-filter doesn't take effect and a so-called "spillover instability" may result, due to the existence of vibration modes. In such cases, the vibration modes cannot be neglected in the controller design procedure. Therefore, the vibration control of high order flexible modes is necessary. The flexible rotor should be modeled as a multi-degree-of-freedom structure, as a notch-filter is not added to the controller, so that the vibration modes can be taken into consideration in the control system design procedure. According to the idea presented above, it is difficult to exactly identify the vibration modes of the flexible rotor, because in the case where the flexible rotor-AMB systems are precisely considered, the equivalent mass, stiffness and the orthogonal modal matrix become complex in shape. One of the authors had presented a method for identifying such complex flexible systems using an iterative modification of the modal matrix. Nevertheless, this method has not been applied to such a complicated system as a flexible rotor.

In this paper, a controller design procedure for a flexible rotor-AMB system is considered. The modeling method presented by Seto is applied in order to obtain an exact multi-degree-of-freedom model of the flexible rotor-AMB system. Utilizing the obtained model, a state equation system model is composed and a feedback gain controller is designed using PID and LQ control laws. It is important to use different control methods for controlling both the rigid and flexible modes. That is, the feedback control of the rigid mode is designed using PID control law, whereas the feedback control of the flexible mode is designed using LQ control law. As the system model includes the multi-degree-of freedom structure model, the designed controller achieves simultaneous motion and vibration control.

Computer simulations are carried out and the effectiveness of the presented procedure is investigated.

2. CONTROL OBJECT

Figure 1 shows a schematic diagram of the flexible rotor used as the control object in this research. The mass of this rotor is about 5.369[kg]. This research considers only the dynamics of the flexible rotor in radial directions, because the PID controller has controlled position of the axial direction. In particular, for the sake of simplicity, this research does not consider the gyroscopic effect of the electric coil.

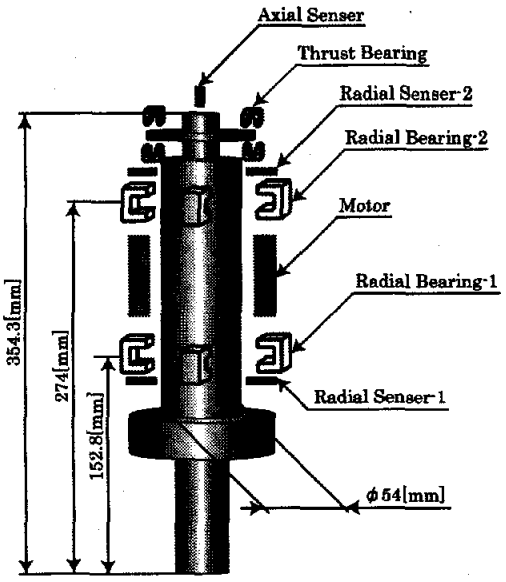

Fig.1 Schematic of flexible rotor-AMB system

3.MAKING REDUCED ORDER PHYSICAL MODEL

3.1 Brief Introduction of Seto's procedure

First, the Seto's method is presented schematically using a 2DOF model as an example.

Generally, the mass matrix, **M**, and the stiffness matrix, **K**, in the physical domain are given by

$$\mathbf{M} = \left(\mathbf{\Phi}\mathbf{\Phi}^{\mathrm{T}}\right)^{-1} \tag{1}$$

$$\mathbf{K} = \left(\mathbf{\Phi}^{\mathrm{T}}\right)^{-1}\mathbf{\Omega}^{2}\mathbf{\Phi}^{-1} \tag{2}$$

Here, $\mathbf{\Phi}$ is the normalized modal matrix, and $\mathbf{\Omega}$ is a diagonal matrix of the natural frequencies of each of the modes.

Because the lumped mass model is not obtained at this stage, the exact value of $\mathbf{\Phi}$ is an unknown quantity. Therefore, a temporarily normalized modal matrix is constructed from the mode shapes shown before.

$$\mathbf{\Phi} = \begin{bmatrix} \phi_{11} & \phi_{12} \\ \phi_{21} & \phi_{22} \end{bmatrix} \tag{3}$$

Because these elements are given from the modal shapes on the distributed parameter system, the temporarily normalized modal matrix constructed from the modal shapes is not guaranteed to satisfy the equation of the mass matrix, where both sides should be diagonal matrices.

$$\mathbf{\Phi}\mathbf{\Phi}^{\mathrm{T}} = \begin{bmatrix} \phi_{11}^2+\phi_{12}^2 & \phi_{11}\phi_{21}+\phi_{12}\phi_{22} \\ \phi_{11}\phi_{21}+\phi_{12}\phi_{22} & \phi_{21}^2+\phi_{22}^2 \end{bmatrix} \neq \begin{bmatrix} \frac{1}{M_1} & 0 \\ 0 & \frac{1}{M_2} \end{bmatrix} \tag{4}$$

Therefore, at first, the non-diagonal elements are defined as the error function ε, given by

$$\varepsilon = \phi_{11}\phi_{21} + \phi_{12}\phi_{22} \tag{5}$$

Then, the sensitivity matrix of the error function in terms of $\mathbf{\Phi}$ can be written as

$$\left\{\frac{\partial\varepsilon}{\partial\mathbf{\Phi}}\right\} = \left\{\frac{\partial\varepsilon}{\partial\phi_{11}} \quad \frac{\partial\varepsilon}{\partial\phi_{12}} \quad \frac{\partial\varepsilon}{\partial\phi_{21}} \quad \frac{\partial\varepsilon}{\partial\phi_{22}}\right\} \tag{6}$$

The modification vector for $\mathbf{\Phi}$, which reduces the error function to zero, is represented as

$$\left\{\frac{\partial\varepsilon}{\partial\mathbf{\Phi}}\right\} = \begin{Bmatrix} \delta\phi_{11} \\ \delta\phi_{21} \\ \delta\phi_{12} \\ \delta\phi_{22} \end{Bmatrix} = -\varepsilon \tag{7}$$

$$\begin{Bmatrix} \delta\phi_{11} \\ \delta\phi_{21} \\ \delta\phi_{12} \\ \delta\phi_{22} \end{Bmatrix} = \left\{\frac{\partial\varepsilon}{\partial\mathbf{\Phi}}\right\}^{T}\left[\left\{\frac{\partial\varepsilon}{\partial\mathbf{\Phi}}\right\}\left\{\frac{\partial\varepsilon}{\partial\mathbf{\Phi}}\right\}^{T}\right]^{-1}(-\varepsilon) \tag{8}$$

By using this modification vector and iterating the error function, it tends toward zero. So, the expected normalized modal matrix, $\mathbf{\Phi}$, is obtained.

$$\phi_{ij} + \delta\phi_{ij} \rightarrow \phi_{ij} \tag{9}$$

The mass matrix, **M**, and the stiffness matrix, **K**, in the physical domain are then determined.

In this way, the reduced order model is constructed using this method from the normalized modal matrix and the natural frequencies.

3.2 Reduced order model of the rotor-actuator system

In this section, the experimental rotor-actuator system is modeled using Seto's procedure.

The modal shapes and their natural frequencies associated with the rotor obtained by finite element analysis using MSC.NASTRAN are shown in Figure 2. In this study, we consider that the first three modes are to be controlled. Therefore, a three-degree-of-freedom (3DOF) reduced order model is required. The bottom of the rotor and the supported points of the actuators in the thrust direction, which are selected as the modeling

points, are shown in Figure 3. In this study, the control of the flexible rotor is of particular interest. Therefore, in this analysis, the control forces of the AMB are treated as the servo stiffness: $ks1$ and $ks2$.

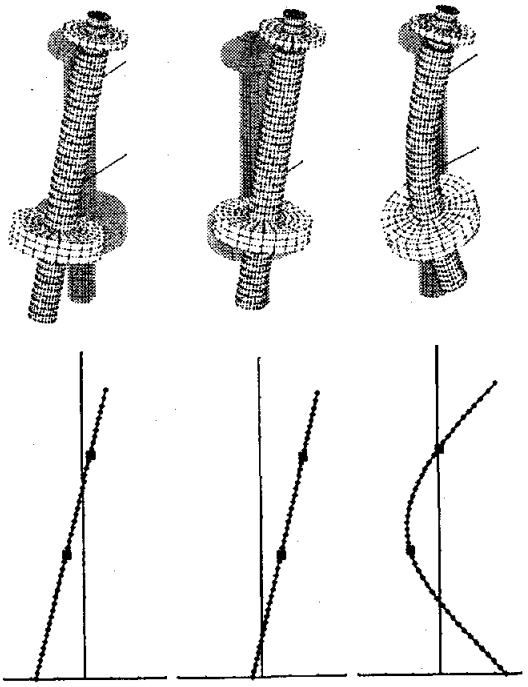

1st mode	2nd mode	3rd mode
11.25[Hz]	27.06[Hz]	1244[Hz]

Fig.2 Vibration mode shapes

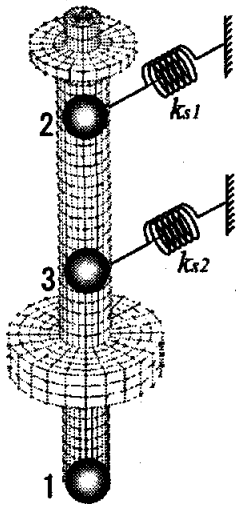

Fig.3 Modeling points

Using the method for constructing the reduced order model, a 3DOF reduced order model of the control object was constructed and is shown in Figure 4.

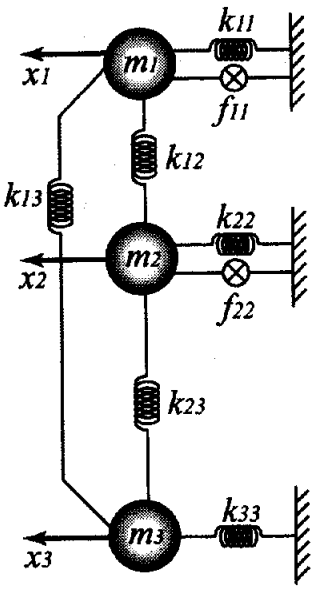

Fig4. Reduced Order Physical Model

The physical parameters are shown as follows. Here, f_{11} and f_{22} are the controlling forces by the AMB.

$$\begin{cases} m_1 = 1.796\ [kg] \\ m_2 = 2.485\ [kg] \\ m_3 = 0.4590[kg] \end{cases}, \quad \begin{cases} k_{11} = -0.1901\times10^7\ [N/m] \\ k_{12} = 1.833\times10^7\ [N/m] \\ k_{13} = -1.0146\times10^7\ [N/m] \\ k_{22} = 0.5808\times10^7\ [N/m] \\ k_{23} = 2.986\times10^7\ [N/m] \\ k_{33} = -0.3194\times10^7\ [N/m] \end{cases}$$

4. CONTORL SYSTEM DESIGN

In this section, the design of a control system for a flexible rotor-AMB system model obtained in the former section is carried out. Firstly, the PID control law that controls the two rigid modes (parallel and comical) is applied to the system model. Then, LQ control law that controls the flexible modes is applied.

4.1 State Equation of Control Object

According to the former section, the state equation of the control object is given as:

$$\dot{\boldsymbol{X}}_c = \boldsymbol{A}_c\boldsymbol{X}_c + \boldsymbol{B}_c\boldsymbol{u}_c \tag{10}$$

$$\boldsymbol{Y}_c = \boldsymbol{C}_c\boldsymbol{X}_c \tag{11}$$

$$\boldsymbol{X}_c = \{\dot{x}_1 \quad \dot{x}_2 \quad \dot{x}_3 \quad x_1 \quad x_2 \quad x_3\}^T$$

The coefficient matrices A_c, B_c, and C_c are given by

$$A_c = \begin{bmatrix} 0_{3\times3} & A_{12} \\ I_{3\times3} & 0_{3\times3} \end{bmatrix}$$

$$A_{12} = \begin{bmatrix} \frac{-(k_{11}-ks1)-k_{12}-k_{13}}{m_1} & \frac{k_{12}}{m_1} & \frac{k_{13}}{m_1} \\ \frac{k_{12}}{m_2} & \frac{-k_{12}-(k_{22}-ks2)-k_{23}}{m_2} & \frac{k_{23}}{m_2} \\ \frac{k_{13}}{m_3} & \frac{k_{23}}{m_3} & \frac{-k_{13}-k_{23}-k_{33}}{m_3} \end{bmatrix}$$

$$B_c = \begin{bmatrix} \frac{1}{m_1} & 0 & 0 & 0 & 0 & 0 \\ 0 & \frac{1}{m_2} & 0 & 0 & 0 & 0 \end{bmatrix}^T$$

$$C_c = \begin{bmatrix} 0 & 0 & 0 & 1 & 0 & 0 \\ 0 & 0 & 0 & 0 & 1 & 0 \end{bmatrix}$$

Here, k_{11} and k_{22} in matrix A_{12} include the servo stiffness. The $ks1$ and $ks2$ are therefore reduced.

4.2 PID control

In this study, using PID control stabilizes the system. The two rigid modes are also controlled. Figure 5 shows the associated block diagram.

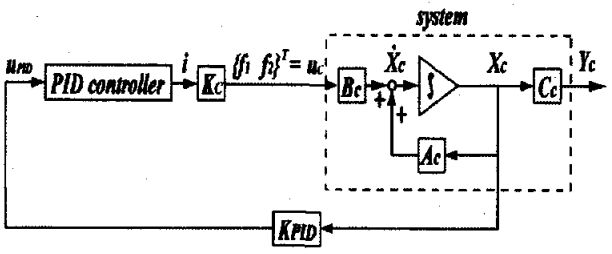

Fig.5 Block diagram

The transfer function from i to u is designed. This is given by

$$\frac{i}{u_{PID}} = \left(\frac{T\alpha s+1}{Ts+1}\right)\left(\frac{T\alpha s+1}{Ts+1}\right) \tag{12}$$

Furthermore, it can be shown that

$$\frac{i}{e}\cdot\frac{e}{u_{PID}} = \frac{T^2\alpha^2 s^2+2T\alpha s+1}{T^2 s^2+2Ts+1} \tag{13}$$

Here, Fig.5 shows that

$$f_{11} = K_c i_{11} \quad , \quad f_{22} = K_c i_{22}$$

and

$$u_{PID} = \{u_{1PID} \quad u_{2PID}\}^T$$

According to the equation shown above,

$$f_{11} = 2K_cT\alpha(1-\alpha)\dot{e}+K_c(1-\alpha^2)e+K_c\alpha^2u_{1PID} \tag{14}$$

$$f_{22} = 2K_cT\alpha(1-\alpha)\dot{e}+K_c(1-\alpha^2)e+K_c\alpha^2u_{2PID} \tag{15}$$

and

$$\ddot{e}_1 = -\frac{2}{T}\dot{e}_1-\frac{1}{T^2}e_1+\frac{1}{T^2}u_{1PID} \tag{16}$$

$$\ddot{e}_2 = -\frac{2}{T}\dot{e}_2-\frac{1}{T^2}e_2+\frac{1}{T^2}u_{2PID} \tag{17}$$

4.3 Augmented system

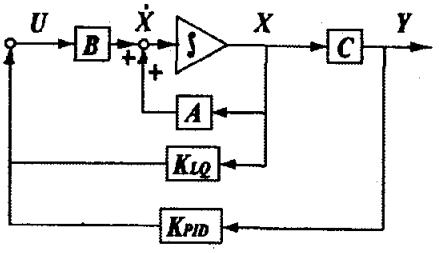

Fig.6 Block diagram of augmented system

Figure.6 shows a block diagram of the control system based on the combined PID and LQ control systems. The feedback gain vectors, $\mathbf{K}_{PID}$ and $\mathbf{K}_{LQ}$, are obtained simultaneously by applying LQ control law to the augmented system. According to Figure 6, the state equation and output equation are given by

$$\dot{X} = AX + BU \tag{18}$$

$$Y = CX \tag{19}$$

Here,

$$X = \{\dot{x}_1 \quad \dot{x}_2 \quad \dot{x}_3 \quad x_1 \quad x_2 \quad x_3 \quad \dot{e}_1 \quad \dot{e}_2 \quad e_1 \quad e_2\}^T$$

and

$$U = -\left(K_{PID}C + K_{LQ}\right)X$$

The coefficient matrices are given by

$$A = \begin{bmatrix} 0_{3\times3} & A_{12} & A_{13} \\ I_{3\times3} & 0_{3\times3} & 0_{3\times4} \\ 0_{4\times3} & 0_{4\times3} & A_{33} \end{bmatrix}$$

$$A_{13}=\begin{bmatrix} \frac{2K_cT\alpha(1-\alpha)}{m_1} & 0 & \frac{K_c(1-\alpha^2)}{m_1} & 0 \\ 0 & \frac{2K_cT\alpha(1-\alpha)}{m_2} & 0 & \frac{K_c(1-\alpha^2)}{m_2} \\ 0 & 0 & 0 & 0 \end{bmatrix}$$

$$A_{33}=\begin{bmatrix} -\frac{2}{T} & 0 & -\frac{1}{T^2} & 0 \\ 0 & -\frac{2}{T} & 0 & -\frac{1}{T^2} \\ 1 & 0 & 0 & 0 \\ 0 & 1 & 0 & 0 \end{bmatrix}$$

$$B=\begin{bmatrix} \frac{K_c\alpha^2}{m_1} & 0 & 0 & 0 & 0 & 0 & \frac{1}{T^2} & 0 & 0 & 0 \\ 0 & \frac{K_c\alpha^2}{m_2} & 0 & 0 & 0 & 0 & 0 & \frac{1}{T^2} & 0 & 0 \end{bmatrix}^T$$

$$C=\begin{bmatrix} 0 & 0 & 0 & 1 & 0 & 0 & 0 & 0 & 0 & 0 \\ 0 & 0 & 0 & 0 & 1 & 0 & 0 & 0 & 0 & 0 \end{bmatrix}$$

5. COMPUTER SIMULATION

5.1 PID control

The simulation shows the frequency responses using PID control law. As examples, the responses at mass point 1 are shown in Figure 7. The gray lines represent the uncontrolled responses while the black lines represent the controlled responses. In Figure 7, the frequency responses from the control command to the displacement at mass point 1 are shown. It is clearly shown that the 1st and 2nd rigid modes are well suppressed. However, the 3rd flexible mode is not suppressed. This is because PID control law is used for controlling the 1st and 2nd rigid modes in this study.

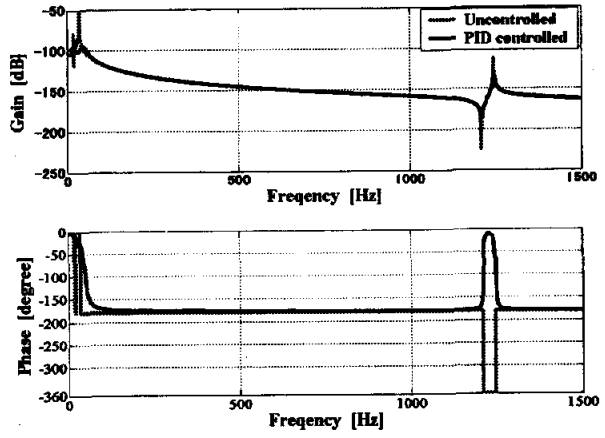

Fig.7 Frequency Response

5.2 PID and LQ control

The simulation shows the frequency response using the controller based on the combined PID and LQ control laws. As an example, the responses at mass point 1 are shown in Figure 8. The same legend applies here as for the equivalent figure shown in the previous section. In Figure 8, the frequency responses from the control command to the displacement at mass point 1are shown. It is clearly shown that the 3rd flexible mode is well suppressed by applying the controller based on the combined PID and LQ control laws. Good control performance is achieved by this controller.

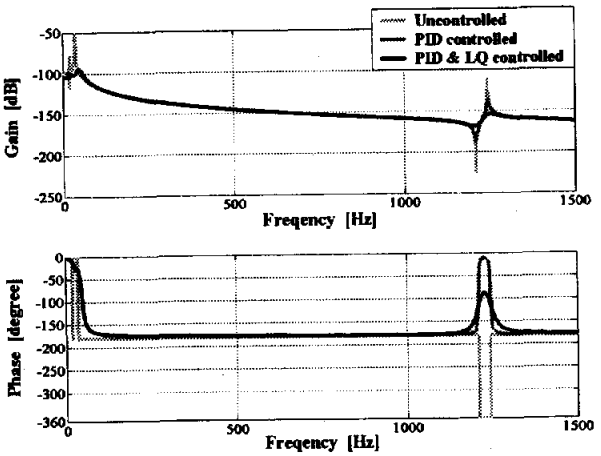

Fig.8 Frequency Response

6. CONCLUSIONS

In this paper, a controller design procedure for a flexible rotor-AMB system is investigated. The modeling method presented by SETO is applied in order to obtain an exact multi-degree-of-freedom model of the flexible rotor-AMB system model. Utilizing the obtained model, a state equation system model is composed and a feedback controller is designed using PID and LQ control laws. Figure 8 clearly shows that all resonance peaks are well suppressed by applying this controller. However, in this simulation, the control performances for the 1st and 2nd modes are similar.. This is because the feedback gain by PID control law is too large.

Computer simulations are carried out and the effectiveness of the presented procedure is confirmed.

REFERENCES

[1] Seto K., and Mitsuda S., Anew Method for Making A Reduced-order Model of Flexible Structures Using Unobservability and Uncontrollability and Its Application in Vibration Control, JSME Int. J., Ser. C, 37-3, 444-449, (1992).

[2]Kijimoto S., Nagamatsu A., Seto K., Kanemitsu Y., Vibration Control of the Structure with an Active Mechanical Component, JSME Int. J., Ser. Ⅲ, 33-3, 441-445, (1990)

[3]Weimin CUI and Nonami K., H_∞ Control of Flexible Rotor-Magnetic Bearing Systems, JSME, Ser. C, 58-553, 56-62, (1992) (in Japanese)

[4]C. W. Lee, Y. K. Yoon, H. S. Jeong, Compensation of Tool Axis Misalignment in Active Magnetic Bearing Spindle System, Proc.of the 3rd Int. Conference on Motion and Vibration Control, Vol 1, 134-139, (1996)

[5]Hirata M., Kamei M., Nonami K., Robust Digital Control of A Magnetic Bearing System Using Sampled-Data H_∞ Control, Proc.of the 4th Int. Conference on Motion and Vibration Control, Vol 2, 417-421, (1998)

[6]Saito T., Okada Y., Nagai B., Shinoda Y., Development of Cardan Angle Control Magnetic Bearing and Application to Stabilize Flexible Rotor, JSME, Ser. C, 65-629, 76-81, (1999) (in Japanese)